International Journal of Current Engineering and Technology
E-ISSN 2277 – 4106, P-ISSN 2347 – 5161

Available at http://inpressco.com/category/ijcet

Research Article

Studies on Dielectric, P-E Loop Measurements and Pl Spectra Analysis of BFO-NFO, BFO-CFO, BFO-ZFO (Perovskite-Spinel) Nanocomposites Prepared by Solution Method

Soumya Mukherjee

Amity School of Engineering and Technology, Amity University, Kolkata-700156, India

Accepted 10 March 2017, Available online 15 March 2017, **Vol.7, No.2 (April 2017)**

Abstract

Solution chemistry is utilized to synthesize three perovskite-spinel nanocomposites at optimized conditions. PL spectral analysis is carried to observe luminescence of the above synthesized nanocomposites after excitation at same Laser light intensity (Xe Laser, 150 W) at constant scanning rate in Spectrofluorometer. Excitations are observed to be about 250 nm with variable peak intensities for three different nanocomposites and also observed to be different with respect to individual perovskite, spinel phases. BFO-NFO exhibits intermediate PL intensity, whereas BFO-CFO have highest intensity level and that of BFO-ZFO is observed to have the lowest intensity among the three nanocomposites. Dielectric measurements have shown space charge polarization of these samples in terms of loss tangent and Cole-Cole plot. It is primarily related to Maxwell-Wagner type interfacial polarizations arising from prominent grain boundary contributions due to nanocrystalline sizes of respective phases. P-E loop analyses of the most prominent results are analysed to realize the presence of ferroelectric nature among the three nanocomposites. Among the three nanocomposites, BFO-NFO is lossy capacitor, non-linear ferroelectric nature, BFO-CFO lossy capacitor, resistive one while that of BFO-ZFO towards hard ferrite type behaviour.

Keywords: *Perovskite-Spinel, PL spectra, Dielectric, P-E loop*

Introduction

Ceramic nanocomposites based on perovskite-spinel ferrites are gaining importance in modern engineering and scientific applications with prominent versatility in domains like memory devices, catalyst, optical-memory switching, photo-induced devices, multistate memory system etc (Robert C. Pullar). Extensive researches have been reported on experimental observations focused on transitional metal doped perovskite Bismuth Ferrite (Bing Luo *et.al*., Xiaolong Yan *et.al*, Amit Kumar *et.al*.] at Fe (B) site and rare-earth metal at Bi (A) site (Amit Kumar *et.al*.). Most prominent route to synthesize such materials are mainly focussed on solid-state reactions (J Li *et.al*, Matjaz Valant *et.al*], sol-gel technique (K Sen *et.al*, Manoj Kumar *et.al*), hydrothermal technique (Xiaolong Yan *et.al*, Yi Du *et.al*), solution combustion [K Sen] etc. Most of the research articles have shown experimental and theoretical work carried on the evaluation of optical property and band gap for single phase perovskite and spinel based simple ferrites. Experimentally, researchers have evaluated optical properties and band gap for nanocrystalline Nickel Ferrite powder and film using Tauc relation with band gap observed to be quite high around 5eV and 5.7eV. Band gap of nanocrystalline Nickel Ferrite depending on the synthesis is found to vary with thickness of film to a certain extent (Gagan Dixit *et.al*., Manish Srivastava *et.al*.). Band energy transitions for both bulk and nanocrystalline Bismuth Ferrite is evaluated and reported by researchers (G Catalan *et.al*, A Mukherjee *et.al*). Blue emissions around 454nm and weak green emissions around 518nm are noted from PL analysis of Mn doped Bismuth Ferrite due to self activation. Light emissions are mainly attributed to Mn^{+2} co-ordinations attributed to transition of $3d^5$ orbital electrons (Yu Xeulian *et.al*).

In the present investigations, studies on PL spectra for luminenscence, dielectric measurements and effect of polarizibility with applied external fields at various frequencies and gradients are applied for three nanocomposites based on equimolar Perovskite-Spinel synthesized by solution method.

Experimental Procedure:

Precursors used are AR grade of Bismuth nitrate pentahydrate (Merck India), Ferric nitrate nonahydrate (Merck India), Ethylene Glycol, Acetic acid

*Corresponding author: **Soumya Mukherjee**

for perovskite Bismuth ferrite synthesis. Cobalt nitrate, Nickel nitrate, Ferric nitrate, Zinc nitrate are used respectively as a precursor salt for spinel cobalt ferrite, nickel ferrite and zinc ferrite along with ammonium hydroxide to undergo coprecipitation for the synthesis of above mentioned materials. Nanocomposites are prepared maintaining 1:1 molar ratio of respective individual ferrites (Perovskite:Spinel). Details of synthesis are given in our previous research articles Soumya Mukherjee *et.al*. (2013) & (2014). PL spectral analysis for luminescence are recorded by Spectrofluorometer (ELICO, SL-174) having Xe 150W laser lamp for excitation. Dielectric analysis are carried out by dielectric analyzer till 10^5 Hz (Hioki, 3522-50LCR Hitester) on samples in pellet form having 12mm diameter with high pure Ag paste applied on both sides for conductivity of the samples. Two Cu wires (free from rust) are attached diametrically on both opposite sides of the pellet face to establish the electrical connectivity. Polarization-Electric Field responses are observed at various electrical gradients, frequency applied on the synthesized samples to observe the nature of responses of electric polarization of the synthesized samples. It is measured by Automatic P-E loop tracer (Marine India, Pvt Ltd) at 50Hz with prepared pellets similar to dielectric measurement of the synthesized materials.

Results & Discussions

3.1. PL Spectra (FluorometricAnalysis)

Fluorometric analysis (PL) study is carried out on samples having higher purity of phases developed at respective experimental conditions. PL spectra analyses for all three nanocomposites are measured in fluorometric spectrometer (Sl-174, Elico) using 150W Xe laser lamp with spectral resolution at constant excitation wavelength of 250nm. Two emission peaks, one at 304nm and other at 381nm are observed corresponding to 4.09eV & 3.27eV respectively for BFO-NFO (Fig-1). Recombination rate among excited electrons and holes is considerable leading to PL emission spectra but it is lower than BFO-CFO nanocomposite. Moreover emissions obtained for constant excitation is mostly in the UV region with slight perturbation towards visible range. Intensity of PL spectra peak of the nanocomposite (BFO-NFO) is found to be intermediate between Bismuth Ferrite-Cobalt Ferrite and Bismuth Ferrite-Zinc Ferrite. Intensity of inverse spinel Nickel ferrite is found to be higher than perovskite Bismuth ferrite and also observed to be higher by 5-7 times than equimolar perovskite-inverse spinel Bismuth ferrite-Nickel ferrite nanocomposite. Above nature of PL spectra of the nanocomposite is found to be similar to PL results of (Mohit kumar *et.al*). Two corresponding emission peaks at 304nm and 388.7nm are observed for BFO-CFO nanocomposite. Similar, to previous one it corresponds to band transition energies of 4.09eV & 3.2eV respectively for BFO-CFO nanocomposite synthesized at 550 for 4hours. Intensity of inverse spinel Cobalt ferrite is found to be lower than perovskite Bismuth ferrite and observed to be higher by 3-4 times than equimolar perovskite-inverse spinel Bismuth ferrite-Cobalt ferrite nanocomposite. This result of PL spectra of the nanocomposite is in correspondence to PL observations of Kumar Mohit *et.al*. PL spectra behavior of nanocomposite BFO-ZFO is found to be quite similar in nature to those of individual ferrites, but intensity of emission spectra is found to be quite lower. The PL spectra arises due to deep and shallow hole defects which arises mainly due to the oxygen vacancies created in tetrahedral and octahedral sites. The deep holes are related to large concentration of defects leading to green-red-yellow emission while shallow holes are due to low concentration of defects giving rise to violet-blue emissions. (Mohit Kumar *et.al*.) Ying-Hao *et.al* studied the PL spectra by providing excitation at different wavelengths to observe the effect of Ni substitution on Bismuth Ferrite. Nature of the curves is found to be quite similar to earlier reported publications (Hao Wang *et.al*.). For pure BFO, transition arises from band to band causing intrinsic emission. Any other emission from other higher wavelengths may arise due to defects or impurity giving rise to dopant levels within the band gap (Hao Wang *et.al*) Small hump peak of lower intensity in PL spectra arises for both BFO-NFO and BFO-CFO possibly due to net polarization and grain boundary polarization of both ferrites in the nanocomposite. Thus we observe that among the present nanocomposites, equimolar Bismuth Ferrite-Zinc Ferrite have poor luminenscence property in compare to individual ferrite components as well as lowest intensity of luminenscence among all three nanocomposites.

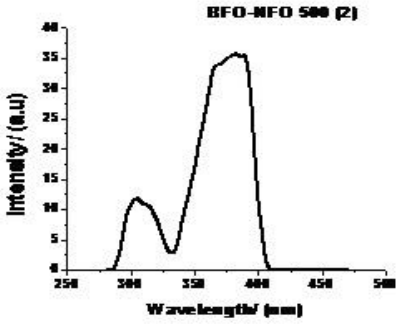

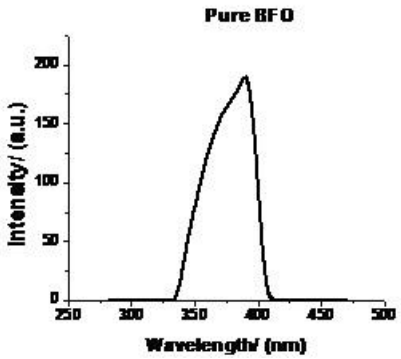

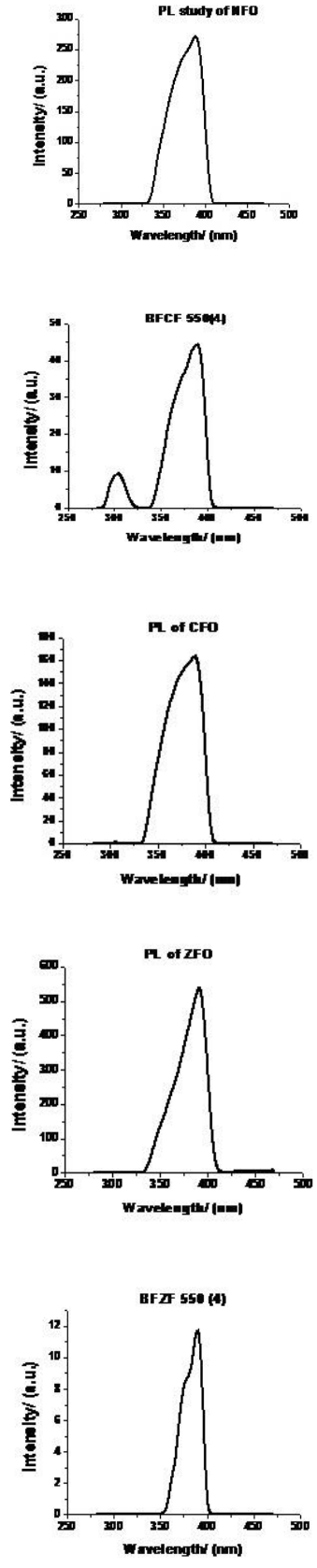

Fig.1 Fluorometric spectra (PL) of BFO-NFO, BFO-CFO, BFO-ZFO nanocomposites, after heat treatment at 500˚C for 2hrs, 550ºC for 4hrs vs. perovskite-nanocrystalline BFO (Bismuth ferrite), spinel nanocrystalline NFO (Nickel ferrite), CFO (Cobalt ferrite) and ZFO (Zinc ferrite)

Dielectric Property Analysis

The Fig. 2 corresponds to Tan delta loss, Relative Permittivity Vs Frequency variations along with Cole-Cole plot to exhibit effect of both imaginary and real impedance measured on the samples till the frequency range of 10^5Hz. Decreasing tan delta or dielectric loss, relative permittivity with variation in frequency due to lagged responses of charged electrical mass to electric field due to inertia factor is found to be possible for space charge polarization. Presence of two different structures are verified from XRD study and crystallite size estimation by Scherrer's formula justified them as nanocomposite having planes of orientation or facets in the direction of growth with minimum energy leading to thermodynamic phase stability. Thus, the polarization behavior of the nanocomposite would be influenced by both structures and phases to a great extent. Dielectric polarization response of perovskite structure is different from that of spinel structure material. In the present experimental article, crystallization of perovskite is more than spinel though equimolar quantities are added. Polarization of the dipoles at the boundary of two different phases have some response which lags due to inertia of masses of charged particles on application of electrical field with variation in frequency giving rise to the possible explanations for the resultant curves. These observations are on the basis of dipole relaxation where the electrical dipoles are incapable to switch with frequency of the applied electric field. In the present case ferromagnetic and ferroelectric-antiferromagnetic based materials are surrounding each other or in contact with each other. These two systems have different structure, permittivity and conductivity. Thus on application of electric field with frequency, space charge produce by one could possibly be impeded by the other phase system of the nanocomposite. As a result some interface polarization arises which follows Maxwell-Wagner type of interfacial polarization.

Moreover, perovskite component have some oxygen defects which may give rise to certain space charge polarization. (M A Ahmed *et.al*.) Values for dielectric loss are 0.15 at lower frequency and 0.03 at highest frequency while the corresponding values for relative permittivities are about 97.5 and 82.5 respectively for BFO-NFO. Permittivity is observed to be constant at about 60000Hz and same noted for dielectric loss with frequency. Recently, Amit Kumar and Hemant Singh *et.al*. have worked on the nanocomposite of $BiFeO_3$-$NiFe_2O_4$ with variations of Ni-ferrite content. They observed that dielectric constant, tanδ increases and decreases with the addition of nickel ferrite content. Similar trend is observed for our sample which consists of equimolar ratio of perovskite-spinel system in contrast to previous research findings where perovskite components are major than spinel component. (M A ahmed *et.al*., Amit Kumar *et.al*., Hemant Singh *et.al*.) Values for dielectric loss is about 0.6 at lower

frequency and approaches about 0.01 at highest frequency while the corresponding values for relative permittivities are about 34 and 12 respectively for BFO-CFO. Constant values of relative permittivity are observed above 60000Hz and same for dielectric loss with frequency. The nature of the curve is found to be in correspondence with the experimental findings from Manoj Kumar *et.al*. Amit Kumar (2013) *et.al*. and Hua-Li Mo *et.al*. Values for dielectric loss is 0.047 at lower frequency and 0.007 at highest frequency while the corresponding values for relative permittivities are about 84.45 and 81.54 respectively for BFO-ZFO. Curve obtained are found to be in close nature with findings of Poonam Uniyal *et.al*. Dielectric constant also corresponds to spontaneous polarization where complex dielectric constant expressed by the following relationship

$$\varepsilon=\varepsilon_o + \varepsilon_s - \varepsilon_o/1 + i\omega\tau \quad \text{(Eq 1)}$$

Complex dielectric is divided into two components a) real and b) imaginary component as

$$\varepsilon' = \varepsilon_o + \varepsilon_s - \varepsilon_o/1 + \omega^2\tau^2 \quad \text{(Eq2)}$$

and

$$\ddot{\varepsilon} = (\varepsilon_s - \varepsilon_o)\omega\tau/1 + \omega^2\tau^2 \quad \text{(Eq3)}$$

(W. D. Kingery *et.al*.)

Relative permittivity is noted to be about 300, 400, 500 while tanδ values are around about 1 as observed by Amit Kumar *et.al* (2013) for Ni substitution on Bismuth Ferrite system while value is about 380 from research paper published by Hemant singh *et.al*. It is noted from previous report that electrical conductivity for spinel ferrites is low in comparison to other magnetic materials and hence finds applications in microwave frequencies. Variations in conductivity are mainly explained by Verweys hopping mechanism where conductivity is mainly possible by hopping of electrons of ions of the same element present in more than one state and distributed randomly over crystallographically equivalent sites. The distance between metal ions at (A) site, (B) site and between (A), (B) sites are important for hopping of electrons. Distance between (A-B) sites is higher than (B-B) and hence the probability of hopping of electron is more within (B-B) sites. Thus hopping depends upon distance between the ions and activation energy while the charges are found to move under the influence of electrical charges in presence of electric field. Cole-Cole plot of the equimolar perovskite–inverse spinel nanocomposite is carried to correlate the electrical properties with microstructure where it is also possible to separate the contribution of grain/bulk and grain boundary to the total conductivity of the material system within the frequency range 10^5Hz. Present analysis is carried at slightly lower frequency so complete two semi circles could not be obtained. It arises since both phases are down to nanocrystallite range leading to higher grain surface area as evident from XRD and microstructural characteristics. Microstructure reveals interlocking among perovskite and inverse spinel type which may give rise to better electron conduction overcoming the barrier between the two. Hence, such prominent second portion arises in the Cole-Cole plot. (Ź Lavarević, *et.al*.) Moreover in Cobalt ferrite, hopping of electrons at sufficient optimum temperature inside the sample grain increases with frequency due to short ranged hopping of charge carriers (holes between Co^{2+} - Co^{3+} and electrons between Fe^{2+} - Fe^{3+} via superexchange paths Fe^{2+}-O-Fe^{3+} and Co^{2+}-O-Co^{3+}) respectively present at the B site of the cubic spinel structure. (N. R. Bhowmick) Ac conductivity of spinel Cobalt ferrite is found to be dependent on hole hoping process between Co^{2+} - Co^{3+} ions, and the dynamics of high inertia Co^{2+} - Co^{3+} leads to suppression at higher frequencies. At higher frequencies electron mobility dominates due to large mobility of Fe^{2+}-O-Fe^{3+} ions (less effective mass). Presence of straight line in the plot indicates possible interfacial polarization among the two phases present in the nanocomposite. The concave upward curve indicates some perturbed impedance contribution from the complex microstructure at the grain interfaces. (N. R. Bhowmick)

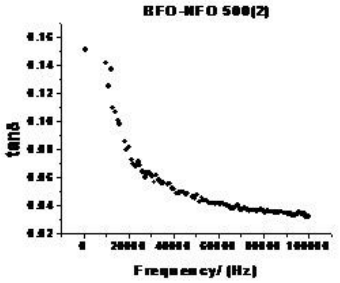

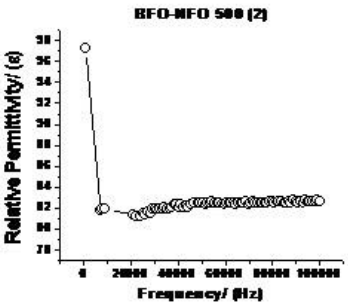

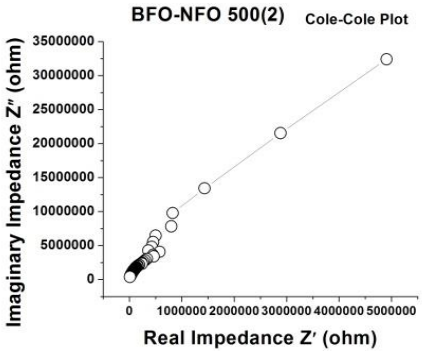

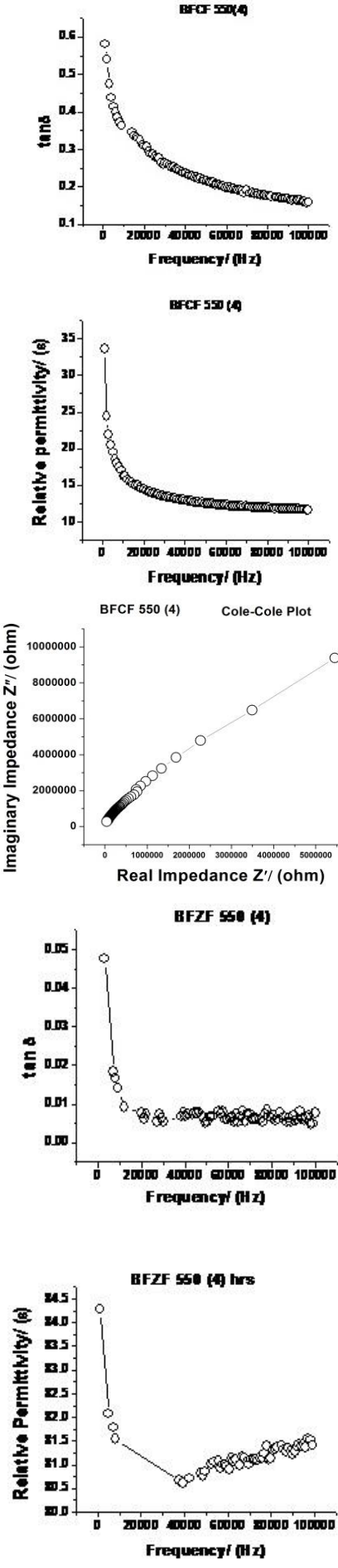

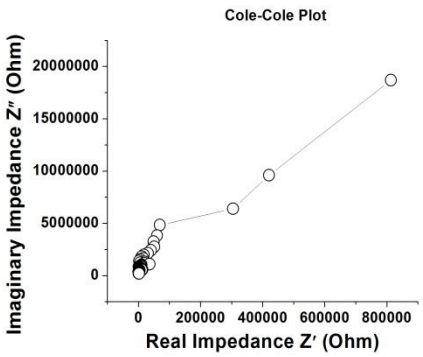

Fig.2 Response of tanδ (Loss tangent) behaviour with frequency, relative permittivity and Cole-Cole plot for BFO-NFO, BFO-CFO and BFO-ZFO nanocomposites heat treated at 500^{0}C for 2hrs, 550ºC for 4hrs.

Polarization-Electric Field Analysis

Polarization Electric Field loop obtained for the present synthesized samples is shown in the Fig. 3. All the figures obtained are performed at different potentials, frequencies and accordingly the responses of the sample in presence of electric field. Responses of the curve for BFO-NFO are in close approximation to lossy capacitor nature while non-linear ferroelectric nature is observed for the present sample consisting of equimolar ratio of perovskite-spinel components of Bismuth ferrite-Nickel Ferrite. The loop observed arises due to possible Maxwell-Wagner interfacial polarization and contribution of space charge polarization from the possible oxygen vacancy present within perovskite component Bismuth Ferrite of the nanocomposite. The area under the curve is noted to vary at different gradient at various frequencies depending upon the response of the dipole and electrical domains with frequency of the applied electric field. Similar close nature P-E loop curves are also reported for Bismuth ferrite ceramics due to domain wall pinning effect by Tadej Rojac *et.al*. In the present composites pinning arise at the interface of the boundary between perovskite and spinel component.

Break down voltage for the equimolar Bismuth ferrite-Nickel ferrite nanocomposite (BFO-NFO) obtained at 1 Hz frequency is 4KV/mm. Loss character is found to be proportional with area under the curve. For different samples at 1000Hz 500V/mm, 1000Hz 3KV/mm, 10Hz 2KV/mm, 100Hz 2KV/mm, 10Hz 3.5KV/mm, 100Hz 3.5KV/mm typical features obtained from the P-E loop are shown in Table I. Loss obtained for sample BFO-NFO is highest at 1Hz 2KV/mm. It is also noted that loss reduces at higher frequency and also with higher voltage gradient due to possible polarizing of charges and ferroelectric domains with the applied electrical field.

Table 1 P-E loop parameters for BFO-NFO synthesized at 500°C for 2hrs

Freq (Hz)	V Grad (KV/mm)	Ps (μC/cm²)	Ec (V)	Pr (μC/cm²)	Area (μJ/cm²)
1	2	0.119	(+)1432, (-)1464	0.185	1011.81
10	2	0.058	(+)781.75, (-)927.742	0.036	192.85
10	3.5	0.102	(+)1527.18, ()1750.39	0.064	655.7
100	2	0.0097	(+)333.02, (-)487.967	0.0017	52.7
100	3.5	0.0636	(+)630.53, (-)918.019	0.018	174.073
1000	0.5	0.0066102	(+)43.4, (-)111	0.00155	1.4
1000	3	0.0545	(+)518.85, (-)767.85	0.015	124.347

Ps = Saturation polarization, Ec = Coercive field, Pr = Remnant polarization, V = Voltage gradient on the sample.

For BFO-CFO 550 (4) hrs at 1Hz, 1KV/mm, saturation polarization is 0.005165μC/cm², coercive field in positive and negative coordinate is 6.38V, 28.674V while remnant polarization obtained is Pr (+) = 0.01579μC/cm². The loss obtained from area under the curve is 1.66811μJ/cm². Ferroelectric nature tendency is noted for 1Hz at 1KV/mm. Loss character is found to be proportional with area under the curve. For sample at 10Hz, 2KV/mm coercive field is 1625.94V, 1631.49V in positive and negative gradient while remnant polarization obtained is 0.201μC/cm². Lossy character is observed to increase at higher voltage gradient and at higher frequency in contrast to the previous case. Hence P-E loop behaviour is different under higher electrical gradient and also at higher frequency. It may be due to the possible facts that domains present in the nanocomposite of equimolar BFO-CFO are more magnetic in nature which tries to be aligned more easily with electrical field and difficult to change its alignment when the electrical field is reversed due to inertial effect.

For BFO-ZFO 550 (4) hrs 1Hz, 1KV/mm, coercive field in positive and negative coordinates are 149.523V, 164.75V. Remnant polarization obtained at zero fields is 363.207μC/cm² while saturation polarization is 345.845μC/cm². The loss obtained after the work done due to the response of polarization under the applied electric field is 253202μJ/cm². Coercive field at higher voltage gradient is 165.987V (+) gradient, 185.94V (-) gradient while remnant polarization and saturation polarization noted are 400.494μC/cm², 389.21μC/cm². The loss obtained for the sample is 294845μJ/cm².

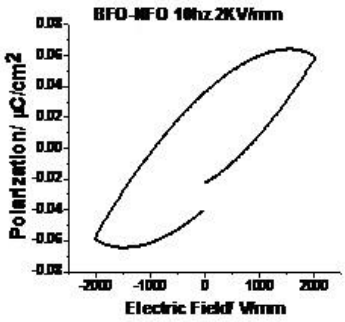

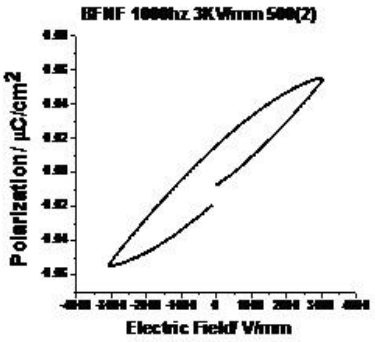

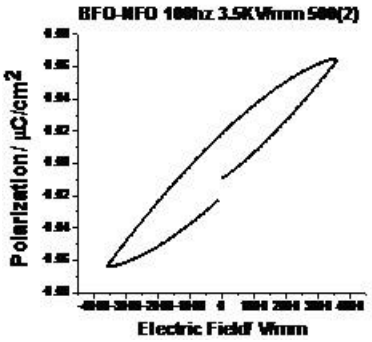

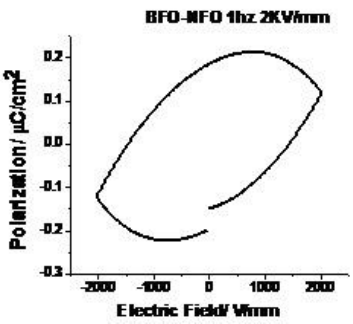

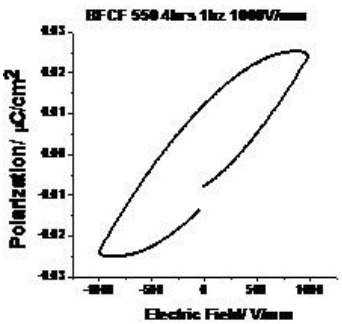

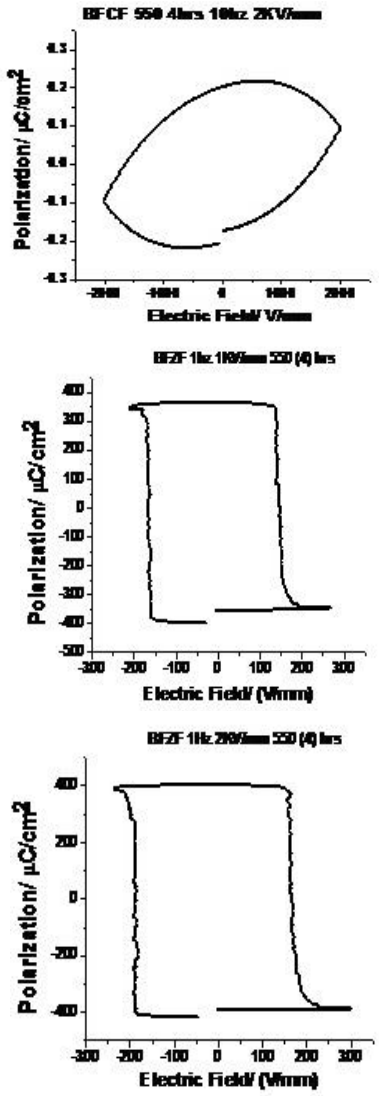

Fig.3. Polarization-Electric Field responses of nanocomposites of BFO-NFO, BFO-CFO and BFO-ZFO synthesized at 500˚C for 2 hours, 550ºC for 4hrs at various frequencies and voltage gradients

Conclusions

Three nanocomposites based on perovskite-spinel is synthesized utilizing solution chemistry. PL spectral analysis is carried to observe luminescence of the above synthesized nanocomposites. Amongst three nanocomposites, BFO-NFO exhibits intermediate PL intensity, BFO-CFO highest and that of BFO-ZFO is observed to be the lowest in behaviour. The PL spectra is observed to be linked with oxygen vacancies created in tetrahedral, octahedral sites of M-O co-ordination which gives rise to deep and shallow holes defects. The deep holes are related to large concentration of defects leading to green-red-yellow emission while shallow holes are due to low concentration of defects giving rise to violet-blue emissions. Dielectric measurements are studied to note space charge polarization nature in terms of dielectric constant, loss tangent and Cole-Cole plot having Maxwell-Wagner interfacial polarization due to prominent grain boundary polarizations for the nanocrystalline sizes of respective phases of Perovskite-Spinel. P-E loop analyses measured on the most prominent samples to realize the ferroelectric behaviour among the three nanocomposites. Among the three BFO-NFO exhibits lossy capacitor, non-linear ferroelectric nature, BFO-CFO lossy capacitor, resistive character while that of BFO-ZFO have hard ferrite type behaviour.

Acknowledgement

I thank the Department of Metallurgical & Materials Engineering, Jadavpur University for providing space to carry the experiments and West Bengal Government Fellowship for supporting work during my PhD tenure.

References

Pullar, C. Robert. (2012), Hexagonal ferrites: A review of the synthesis, properties and applications of hexaferrite ceramics. *Progress in Materials Science,* 57 (7),pp 1191-1334.

Luo, Bing. Cheng., Chen, Le Chang., Xu, Zhi., Xie, Qian. (2010), Effect of Cr substitution on the multiferroic properties of $BiFe_{1-x}Cr_xO_3$ compounds. *Physical Letters A*, 374 (41), pp 4265-4268.

Yan, Xiaolong., Chen, Jianguo., Qi, Yufa., Cheng, Jinrong., Meng, Zhongyan. (2010), Hydrothermal synthesis and characterization of multiferroic $Bi_{1-x}La_xFeO_3$ crystallites. *Journal of the European Ceramic Society,* 30 (2) pp 265-269.

Kumar, Amit., Yadav, K.L. (2011), Magnetic, magnetocapacitance and dielectric properties of Cr doped bismuth ferrite nanoceramics. *Materials Science and Engineering B,* 176 (3) pp 227-230.

Li, J., Duan, Y., He, H., Song, D. (2001), Crystal structure, electronic structure, and magnetic properties of bismuth-strontium ferrite. *Journal of Alloys and Compounds,* 315 (1-2) pp 259-264.

Valant, Matjaz., Axelsson, Karin Anna., Alford, Neil. (2007), Peculiarities of a Solid-State Synthesis of Multiferroic Polycrystalline $BiFeO_3$. *Chemistry of Materials,* 19 (22) pp 5431-5436.

Sen, K., Singh, K., Gautam, Ashish., Singh, M. (2012), Dispersion studies of La substitution on dielectric and ferroelectric properties of multiferroic $BiFeO_3$ ceramic. *Ceramics International,* 38 (1) pp 243-249.

Kumar, Manoj., Yadav, L. K. (2007), Magnetoelectric characterization of $xNi_{0.75}Co_{0.25}Fe_2O_4$-(1-x)$BiFeO_3$ nanocomposites. *Journal of Physics and Chemistry of Solids*. 68 (9) pp 1791-1795.

Du, Yi., Cheng, Yiang Zhen., Shahbazi, Mahboobeh., Collings, W Edward., Miotello, A., Dou, Xue Shi., Wang, Lin. Xiao. (2010), Enhancement of ferromagnetic and dielectric properties of lanthanum doped $BiFeO_3$ by hydrothermal synthesis. *Journal of Alloys and Compounds*, 490 (1-2) pp 637-641.

Dixit, Gagan., Singh, P. J., Srivastava, C. R., Agarwal, M. H., Chaudhary, J. R. (2012), Structural, Magnetic and Optical Studies of Nickel Ferrite Thin Films. *Advanced Material Letters,* 3 (1) pp 21-28.

Srivastava, Manish., Ojha, K. Animesh., Chaubey, S., Materny, A. (2009), *Vacuum,* 481 pp 515-519.

Catalan, G., Scott, F. J. (2009), Physics and Applications of Bismuth Ferrite. *Advanced Materials,* 21 (24) pp2463-2485.

Mukherjee, A., Hossain, M. S., Pal M., Basu, S. (2012), Effect of Y doping on optical properties of multiferroic $BiFeO_3$ nanoparticles. *Applied NanoScience,* 2 (3) pp 305-310.

Xuelian, Yu., Xiaoqiang, An. (2009), Enhanced magnetic and optical properties of pure and (Mn, Sr) doped $BiFeO_3$ nanocrystals. *Solid State Communications,* 149 (17-18) pp 711-714.

Mukherjee, Soumya., Mitra, K. M. (2013), Synthesis and Characterization of Bismuth Ferrite-Nickel Ferrite Nanocomposite. *Interceram,* 62 (5) pp 376-379.

Mukherjee, Soumya., Mitra, K. M. (2014), Characterization of Perovskite-Spinel Nanocomposites (BFO-ZFO) Ferrites Prepared by Chemical Route. *Journal of the Australian Ceramic Society,* 50 (2) pp 180-187.

Kumar, Mohit., Rout, K. S., Parida, S., Singh, P. G., Sharma K. S., Pradhan, K. S., Kim, Won, III. (2011), Structural, optical and dielectric studies of $Ni_xZn_{1-x}Fe_2O_4$ prepared by auto combustion route. *Physica B.* 407 (6) pp 935-942.

Wang, Hao. Ying., Qi, Xiaoding. (2012), The Effects of Nickel substitution on Bismuth Ferrite. *Procedia Engineering.* 36 pp 455-461.

Ahmed, A. M., Mansour, F. S., Afifi, M. (2013), Structural, electric and magnetoelectric properties of $Ni_{0.85}Cu_{0.15}Fe_2O_4/BiFe_{O.7}Mn_{0.3}O_3$ multiferroic nanocomposites. *Journal of Alloys and Compounds*. 578 pp 303-308.

Kumar, Amit., Yadav, L. K. (2010), The effect of Ni substitution on magnetic, dielectric and magnetoelectric properties in $BiFe_{1-x}Ni_xO_3$ system. *Physica B.* 405 (22) pp 4650-4654.

Singh, Hemant., Yadav, L. K. (2014), Synthesis and study of structural, dielectric, magnetic and magnetoelectric characterization of $BiFeO_3$-$NiFe_2O_4$ nanocomposites prepared by chemical solution method. *Journal of Alloys and Compounds*. 585 (February) pp 805-810.

Kumar, Manoj., Yadav, L. K. (2007), Magnetoelectric characterization of $xNi_{0.75}Co_{0.25}Fe_2O_4$-(1-x)$BiFeO_3$ nanocomposites. *Journal of Physics and Chemistry of Solids.* 68 (9) pp 1791-1795.

Kumar, Amit., Yadav, L. K. (2013), Enhanced magnetoelectric sensitivity in $Co_{0.7}Zn_{0.3}Fe_2O_4$-$Bi_{0.9}La_{0.1}FeO_3$ nanocomposites. *Materials Research Bulletin,* 48 (3) pp 1312-1315.

Mo, Li. Hua., Jiang, Mei. Dong., Wang, Mei. Chun., Zhang, Guo. Wei., Jiang, Sen. Ji. (2013), Magnetic, dielectric and magnetoelectric properties of $CoFe_2O_4$-$Bi_{0.85}La_{0.15}FeO_3$ multiferroic properties. *Journal of Alloys and Compounds*. 579 (December) pp 187-191.

Uniyal, Poonam., Yadav, L. K. (2010), Synthesis and Study of multiferroic properties of $ZnFe_2O_4$-$BiFeO_3$ nanocomposite. *Journal of Alloys and Compounds*. 492 (1-2) pp 406-410.

Kingery, D. W., Bowen, K. H., D.R.Uhlmann, R. D. (1976), Introduction to Ceramics. *John Wiley & Sons* (2) p 923-927.

Lavarević, Ź. Zorica., Jovalekić, Čedomir., Sekulić, L. Dalibor., Milutinović, Aleksandra., Baloš, Sebastian., Slankamenac, Miloš., Romčević, Ž. Nebojša. (2013), Structural, electrical and dielectric properties of spinel nickel ferrite prepared by soft mechanochemical synthesis. *Materials Research Bulletin,* 48 (10) pp 4368-4378.

Bhowmik, N. R. (2014), Role of interfacial disorder on room temperature ferromagnetism and giant dielectric constant in nano-sized $Co_{1.5}Fe_{1.5}O_4$ ferrite grains. *Materials Research Bulletin,* 50 pp 476-482.

Rojac, Tadej., Kosec, Marija., Budic, Bojan., Setter, Nava., Damjanovic, Dragan. (2010), Strong ferroelectric domain-wall pinning in $BiFeO_3$ ceramics. Journal of Applied Physics, 108 074107-1 – 074107-8